

*Conference Proceedings Paper*

# Nb-Ta-Ti Oxides in Topaz Granites of the Geyer Granite Stock (Erzgebirge Mts., Germany)

Miloš René

Institute of Rock Structure and Mechanics, v.v.i., Academy of Sciences of the Czech Republic, V Holešovičkách 41, 182 09 Prague 8, Czech Republic; rene@irsm.cas.cz; Tel.: +420-266-009-228

**Abstract:** Nb-Ta-Ti-bearing oxide minerals (Nb-Ta-rich rutile, columbite-group minerals, and W-bearing ixiolite) represent the most common host in high-F, high-P Li-mica granites and related rocks from the Geyersberg granite stock in the Krušné Hory/Erzgebirge Mts. batholith. The Geyersberg granite stock forms a pipe like granite stock composed of fine- to middle-grained, porphyritic to equigranular topaz- Li mica granites, containing up to 6 vol % of topaz. Intrusive breccias on the NW range of the granite stock are composed of mica schists- and muscovite gneiss fragments enclosed in fine-grained aplitic granite. The high-F, high-P<sub>2</sub>O<sub>5</sub> Li-mica Geyersberg granites, which represent the youngest granite intrusions in the Western and Middle Krušné Hory/Erzgebirge plutons, are highly fractionated S-type granites (ASI = 1.2–1.5) with low Nb/Ta ratio (0.9–1.4) and enrichment in Rb (1190–1660 ppm), Cs (28–42 ppm), Nb (33–101 ppm) and Ta (37–76 ppm). Columbite group minerals occur usually as euhedral to subhedral grains that display irregular or patched zoning. These minerals are represented by columbite-(Fe) with Mn/(Mn + Fe) ratio ranging from 0.07 to 0.15. The rare Fe-rich W-bearing ixiolite occurs as small needle-like crystals. The ixiolite is Fe-rich with relatively low Mn/(Mn + Fe) and Ta/(Ta + Nb) values (0.10–0.15 and 0.06–0.20 respectively. Owing to the high W content (19.8–34.9 wt % WO<sub>3</sub>, 0.11–0.20 apfu), the sum of Nb + Ta in the ixiolite does not exceed 0.43 apfu. The Ti content is 1.7–5.7 wt % TiO<sub>2</sub> and Sn content is relatively low (0.3–4.1 wt % SnO<sub>2</sub>).

**Keywords:** topaz granite; Nb-Ta rutile; columbite; ixiolite; Saxothuringian zone

## 1. Introduction

Niobium- and tantalum-bearing oxide minerals are common in topaz granites and related rocks (pegmatites, alkali-feldspar syenites). The most common Nb-Ta-bearing minerals in these parageneses are Nb-Ta-bearing rutile and columbite-group minerals.

In the Krušné Hory/Erzgebirge region these minerals were previously described by Johan and Johan [1], Rub et al. [2] and Breiter [3] from the Cínovec granite cupola, by Breiter et al. [4] from the Podlesí granite stock and by René and Škoda [5] from the Krásno-Horní Slavkov ore district in the Slavkovský les Mts. The Nb-Ta-Ti oxides described in this paper are part of the mineral assemblage in topaz-Li-mica granites from the Geyersberg granite stocks in the middle part of the Krušné Hory/Erzgebirge batholith.

## 2. Geological Setting

The Variscan granitoid rocks in the Krušné Hory/Erzgebirge and Slavkovský les Mts. form a discontinuous belt extending about 160 km along the Czech Republic-Germany border in a NE-SW direction. The belt comprises an area about 6000 km<sup>2</sup> and is positioned near the southern border of the Saxothuringian zone, at the northwestern edge of the Bohemian Massif. These granitoid rocks were successively emplaced in the Late Carboniferous and early Permian and intruded into folded

and metamorphosed lithostratigraphic units consisting of Proterozoic paragneisses, late Proterozoic-Cambrian mica schists and phyllites as well as quartzites of predominantly Ordovician age [6–8].

The Krušné Hory/Erzgebirge batholith consists of three individual plutons: Western, Middle and Eastern, each representing an assembly of shallowly emplaced granite units about 6–10 km paleodepth, with a maximum preserved vertical thickness of the pluton 10–13 km below the present surface level [9,10]. All these granites have been classified in a number of ways in the past [11–16]. The recently mostly used classification of these granites subdivides these granitic rocks into late collisional and post-collisional granites. The late collisional granites were divided into the following three groups (1) low-F biotite granites; (2) low-F two-mica granites and (3) high-F, high-P<sub>2</sub>O<sub>5</sub> Li-mica granites. The post-collisional granites were divided into high-F, low-P<sub>2</sub>O<sub>5</sub> Li-mica granites and medium-F, low-P<sub>2</sub>O<sub>5</sub> biotite granites [6,17].

The Geyersberg granite stock is part of the shallow intrusive granite bodies occurred in the middle section of the Krušné Hory/Erzgebirge batholith. These granite bodies (Vierung, Sauberg, Geyersberg, Ziegelberg and Greifenstein) are located near old mining towns of Ehrenfriedersdorf and Geyer. The occurrence of granite stocks and ridge-shaped apical parts of the Middle Erzgebirge granite pluton is controlled by the NW-SE striking Geyer-Elterlein-Herold shear zone with NE-SW striking faults (systems of the Geyer-Schönfeld, Franzenhöhe Wilischthal and Wiesenbaden faults). These fault systems also facilitated emplacement of microgranite, aplite and lamprophyre dykes in the area. Subsurface morphology of above mentioned granite stocks was investigated by numerous exploration boreholes [18–20] and interpreted using regional gravity measurements [21] (Figure 1).

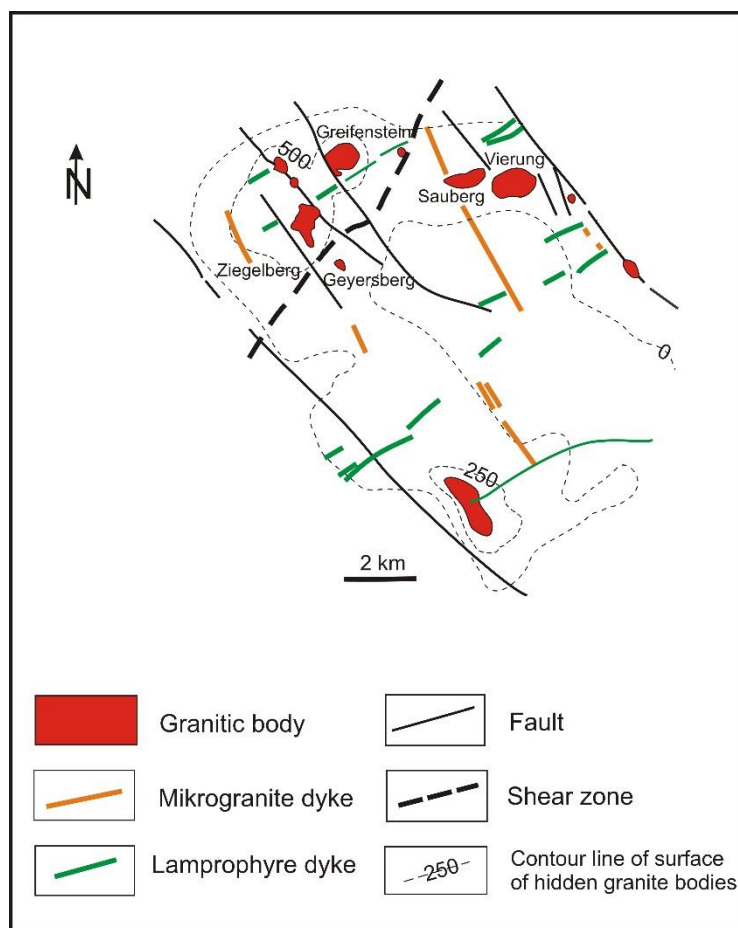


**Figure 1.** Geological map of the Middle part of the Krušné Hory/Erzgebirge batholith, modified after [17].

The Geyersberg granite stock forms a pipe like granite stock composed of fine- to middle-grained, porphyritic to equigranular high-F, high P<sub>2</sub>O<sub>5</sub> Li mica granites, containing usually 2–6 vol %

of topaz. Intrusive breccias on the NW range of the granite stock are composed of mica schists and muscovite gneiss fragments enclosed in fine-grained aplitic granite. Granites are partly greisenised, mainly along steeply dipping NW-SE, and NE-SW trending faults. On the western and eastern margin of the granite stock occur small layers and lenses of marginal pegmatites (stockscheider) (Figure 2).

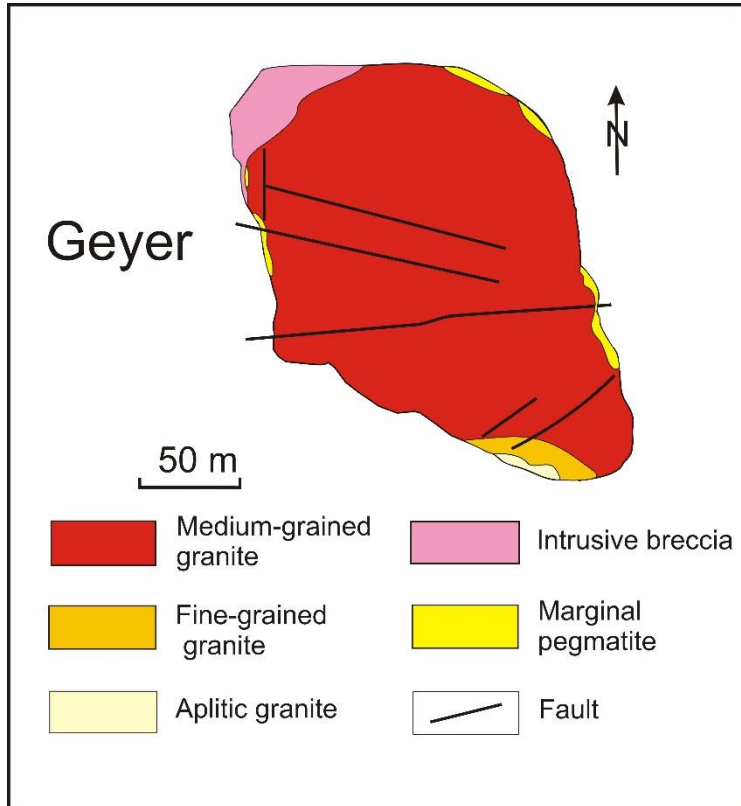


**Figure 2.** Geological map of the Geyersberg granite stock, modified after [19].

### 3. Methods

Approximately 60 quantitative electron-microprobe analyses of Nb-Ta-Ti oxides were performed using five representative samples from the Geyersberg stock. Minerals were analyzed in polished thin sections to obtain information about mineral zoning in the examined rocks. Back-scattered electron images (BSE) were acquired to study the compositional variation of individual mineral grains. The abundances of Al, Bi, Ca, Fe, Mg, Mn, Nb, Sc, Si, Sn, Ta, Ti, U, W, Y and Zr were determined using a

CAMECA SX 100 electron microprobe operated in wavelength-dispersive mode at the Institute of Geological Sciences, Masaryk University in Brno. The accelerating voltage and beam currents were 15 kV and 20 or 40 nA, respectively, with a beam diameter ranging from 1 to 5  $\mu\text{m}$ .

The following standards were used: almandine (Al), metallic Bi (Bi), andradite (Ca, Fe, Si), olivine (Mg), spessartine (Mn), columbite (Nb), synthetic  $\text{ScVO}_4$  (Sc),  $\text{SnO}_2$  (Sn), synthetic  $\text{Ta}_2\text{O}_5$  (Ta),  $\text{TiO}_2$  (Ti), metallic U (U), metallic W (W), synthetic YAG (Y) and zircon (Zr). Peak count-time was 20 s and background time 10 s for major elements, whereas for trace elements they were 40–60 s and 20–30 s, respectively. The raw data were corrected using the PAP matrix corrections [22]. The  $\text{Fe}^{2+}/\text{Fe}^{3+}$  ratio was calculated according to the stoichiometry.

The whole-rock composition of three representative granite samples is presented in Table 1. Major elements were determined by X-ray fluorescence spectrometry using the PANalytical Axios Advanced spectrometer at Activation Laboratories Ltd., Lancaster, ON, Canada. Trace elements were determined by inductively coupled-plasma mass-spectrometry (ICP MS) using a Perkin Elmer Sciex

ELAN 6100 ICP mass spectrometer at Activation Laboratories Ltd. The analytical procedure for ICP MS involves lithium metaborate/tetraborate flux fusion.

**Table 1.** Chemical analyses of high-F, high-P<sub>2</sub>O<sub>5</sub> Li-mica granites of the Geyersberg granite stock.

| Sample                              | 971                    | 1543                         | 1544                         |
|-------------------------------------|------------------------|------------------------------|------------------------------|
| Rock-Type wt %                      | Medium-Grained Granite | Fine-Grained Aplitic Granite | Fine-Grained Aplitic Granite |
| SiO <sub>2</sub>                    | 73.94                  | 74.42                        | 67.14                        |
| TiO <sub>2</sub>                    | 0.01                   | 0.01                         | 0.01                         |
| Al <sub>2</sub> O <sub>3</sub>      | 15.08                  | 15.03                        | 18.73                        |
| Fe <sub>2</sub> O <sub>3</sub> tot. | 1.04                   | 1.28                         | 0.90                         |
| MnO                                 | 0.03                   | 0.03                         | 0.03                         |
| MgO                                 | 0.10                   | 0.04                         | 0.05                         |
| CaO                                 | 0.59                   | 0.51                         | 0.60                         |
| Na <sub>2</sub> O                   | 4.40                   | 3.80                         | 5.68                         |
| K <sub>2</sub> O                    | 3.18                   | 3.54                         | 5.37                         |
| P <sub>2</sub> O <sub>5</sub>       | 0.51                   | 0.55                         | 0.76                         |
| L.O.I.                              | 0.80                   | 1.02                         | 1.10                         |
| Total                               | 99.68                  | 100.23                       | 100.37                       |
| ASI                                 | 1.28                   | 1.37                         | 1.15                         |
| ppm                                 |                        |                              |                              |
| Ba                                  | 30.0                   | 16.0                         | 12.0                         |
| Rb                                  | 1190.0                 | 1390.0                       | 1660.0                       |
| Sr                                  | 54.0                   | 50.0                         | 52.0                         |
| Y                                   | 1.1                    | 0.5                          | 0.5                          |
| Zr                                  | 121.0                  | 14.0                         | 17.0                         |
| Nb                                  | 33.1                   | 92.8                         | 101.0                        |
| Th                                  | 5.8                    | 5.5                          | 13.4                         |
| Ga                                  | 62.0                   | 75.0                         | 96.0                         |
| Zn                                  | 71.0                   | 185.0                        | 98.0                         |
| Hf                                  | 4.2                    | 2.3                          | 3.3                          |
| Cs                                  | 41.8                   | 41.8                         | 28.4                         |
| Ta                                  | 37.1                   | 68.3                         | 76.4                         |
| U                                   | 10.8                   | 19.5                         | 27.1                         |
| La                                  | 1.08                   | 0.11                         | 0.07                         |
| Ce                                  | 2.05                   | 0.21                         | 0.12                         |
| Pr                                  | 0.22                   | 0.04                         | 0.03                         |
| Nd                                  | 0.84                   | 0.15                         | 0.09                         |
| Sm                                  | 0.18                   | 0.07                         | 0.04                         |
| Eu                                  | 0.17                   | 0.02                         | 0.01                         |
| Gd                                  | 0.17                   | 0.07                         | 0.05                         |
| Tb                                  | 0.03                   | 0.01                         | 0.01                         |
| Dy                                  | 0.20                   | 0.06                         | 0.05                         |
| Ho                                  | 0.04                   | 0.01                         | 0.01                         |
| Er                                  | 0.10                   | 0.02                         | 0.01                         |
| Tm                                  | 0.01                   | 0.01                         | 0.01                         |
| Yb                                  | 0.09                   | 0.02                         | 0.02                         |
| Lu                                  | 0.01                   | 0.00                         | 0.00                         |
| La <sub>n</sub> /Yb <sub>n</sub>    | 8.01                   | 3.71                         | 2.36                         |
| Eu/Eu *                             | 2.99                   | 0.70                         | 0.55                         |

#### 4. Results

#### 4.1. Petrology

The main granite variety of the Geyersberg stock consists of high-F, high-P<sub>2</sub>O<sub>5</sub> Li-mica medium-grained granites composed of albite (An<sub>0-1</sub>) (27–35 vol %), quartz (30–34 vol %), K-feldspar (21–30 vol %), Li-mica (4–8 vol %) and topaz (2–6 vol %). Apatite, columbite-group minerals, Nb-Ta-rich rutile, zircon, cassiterite, monazite and uraninite are accessories. Both feldspars are enriched in P (up to 1.2 wt % P<sub>2</sub>O<sub>5</sub>).

The fine-grained aplitic granite, which also forms the groundmass of intrusive breccias contains quartz (32–33 vol %), albite (An<sub>0-1</sub>) (29–32 vol %), K-feldspar (28–30 vol %), Li-mica (2–4 vol %) and topaz (2 vol %). Apatite, Nb-Ta-rich rutile, columbite-group minerals, cassiterite, zircon, ixiolite and very rare uraninite are accessories.

#### 4.2. Geochemistry

The medium grained high-F, high-P<sub>2</sub>O<sub>5</sub> Li-mica granite from the Geyersberg stock is peraluminous S-type granite with aluminium saturation index from 1.2 to 1.5. In comparison with common S-type granites [23] it is enriched in incompatible elements as Rb (1190 ppm), Cs (42 ppm), Sn (229 ppm), Nb (33 ppm), Ta (37 ppm) and W (11 ppm), but poor in Mg (0.05 wt %), Ca (0.6 wt %), Sr (54 ppm), Ba (30 ppm) and Zr (121 ppm). The fine-grained aplitic granite is also enriched in incompatible elements as Rb (1390–1660 ppm), Cs (28–42 ppm), Nb (93–101 ppm) and Ta (68–76 ppm), but poor in Mg (0.04–0.05 wt % MgO), Ca (0.5–0.6 wt % CaO), Sr (50–52 ppm), Ba (12–16 ppm) and Zr (14–17 ppm) (Table 1).

#### 4.3. Mineralogy of the Ti-Nb-Ta Oxide Assemblage

##### 4.3.1. Nb-Ta-Rich Rutile

Rutile is the most common Nb and Ta carrier in the fine-grained aplitic granite. Rutile occurs mostly as inclusions in lithium mica flakes, where it forms subhedral crystals. The majority of examined grains display irregular zoning (Figure 3). These grains contain very low concentrations of Nb (0.3–4.5 wt % Nb<sub>2</sub>O<sub>5</sub>) and Ta (0.02–1.1 wt % Ta<sub>2</sub>O<sub>5</sub>). Tin and W are also present (0.6–2.4 wt % SnO<sub>2</sub>, 0.1–3.6 wt % WO<sub>3</sub>). The examined rutiles have a variable Fe content (0.4–2.1 wt % FeO), but very low Mn concentrations (0.01–0.03 wt % MnO) (Table 2).

**Table 2.** Representative microprobe analyses of Nb-Ta-bearing rutile (wt %).

| Sample                         | 1544-4 | 1544-5 | 1544-6 | 1544-7 | 1544-8 | 1544-12 | 1544-13 | 1544-14 |
|--------------------------------|--------|--------|--------|--------|--------|---------|---------|---------|
| WO <sub>3</sub>                | 0.21   | 0.18   | 1.53   | 0.15   | 0.11   | 3.62    | 0.14    | 1.28    |
| Ta <sub>2</sub> O <sub>5</sub> | 0.05   | 0.05   | b.d.l. | 0.02   | 0.04   | b.d.l.  | 0.05    | 0.03    |
| Nb <sub>2</sub> O <sub>5</sub> | 0.31   | 0.33   | 0.42   | 0.39   | 0.25   | 0.33    | 0.54    | 0.39    |
| TiO <sub>2</sub>               | 97.38  | 96.75  | 92.83  | 97.83  | 97.57  | 91.52   | 97.56   | 95.89   |
| SiO <sub>2</sub>               | 0.03   | 0.03   | 0.02   | 0.05   | 0.03   | 0.04    | 0.03    | 0.06    |
| ZrO <sub>2</sub>               | b.d.l. | 0.00   | 0.06   | b.d.l. | 0.01   | 0.07    | b.d.l.  | 0.02    |
| SnO <sub>2</sub>               | 1.19   | 1.39   | 3.31   | 1.22   | 1.10   | 1.81    | 0.58    | 1.66    |
| Al <sub>2</sub> O <sub>3</sub> | 0.06   | 0.08   | 0.10   | 0.07   | 0.06   | 0.15    | 0.08    | 0.09    |
| Fe <sub>2</sub> O <sub>3</sub> | 0.00   | 0.00   | 0.00   | 0.00   | 0.00   | 0.00    | 0.00    | 0.00    |
| FeO                            | 0.52   | 0.50   | 0.98   | 0.47   | 0.46   | 1.77    | 0.62    | 0.79    |
| MnO                            | 0.01   | 0.00   | 0.01   | 0.02   | 0.00   | b.d.l.  | 0.01    | 0.01    |
| CaO                            | 0.01   | 0.01   | b.d.l. | b.d.l. | 0.00   | 0.01    | 0.02    | 0.01    |
| Total                          | 99.77  | 99.32  | 99.26  | 100.20 | 99.63  | 99.32   | 99.63   | 100.23  |
| O = 2, apfu                    |        |        |        |        |        |         |         |         |
| W <sup>6+</sup>                | 0.00   | 0.00   | 0.01   | 0.00   | 0.00   | 0.01    | 0.00    | 0.00    |
| Ta <sup>5+</sup>               | 0.00   | 0.00   | 0.00   | 0.00   | 0.00   | 0.00    | 0.00    | 0.00    |
| Nb <sup>5+</sup>               | 0.00   | 0.00   | 0.00   | 0.00   | 0.00   | 0.00    | 0.00    | 0.00    |
| Ti <sup>4+</sup>               | 0.98   | 0.98   | 0.96   | 0.98   | 0.99   | 0.95    | 0.98    | 0.97    |

|                                     |      |      |      |      |      |      |      |      |
|-------------------------------------|------|------|------|------|------|------|------|------|
| $\text{Si}^{4+}$                    | 0.00 | 0.00 | 0.00 | 0.00 | 0.00 | 0.00 | 0.00 | 0.00 |
| $\text{Zr}^{4+}$                    | 0.00 | 0.00 | 0.00 | 0.00 | 0.00 | 0.00 | 0.00 | 0.00 |
| $\text{Sn}^{4+}$                    | 0.01 | 0.01 | 0.02 | 0.01 | 0.01 | 0.01 | 0.00 | 0.01 |
| $\text{Al}^{3+}$                    | 0.00 | 0.00 | 0.00 | 0.00 | 0.00 | 0.00 | 0.00 | 0.00 |
| $\text{Fe}^{3+}$                    | 0.00 | 0.00 | 0.00 | 0.00 | 0.00 | 0.00 | 0.00 | 0.00 |
| $\text{Fe}^{2+}$                    | 0.01 | 0.01 | 0.01 | 0.01 | 0.01 | 0.02 | 0.01 | 0.01 |
| $\text{Mn}^{2+}$                    | 0.00 | 0.00 | 0.00 | 0.00 | 0.00 | 0.00 | 0.00 | 0.00 |
| $\text{Ca}^{2+}$                    | 0.00 | 0.00 | 0.00 | 0.00 | 0.00 | 0.00 | 0.00 | 0.00 |
| Total                               | 1.00 | 1.00 | 1.00 | 1.00 | 1.01 | 0.99 | 0.99 | 0.99 |
| $\text{Mn}/(\text{Mn} + \text{Fe})$ | 0.02 | 0.00 | 0.01 | 0.04 | 0.00 | 0.00 | 0.02 | 0.01 |
| $\text{Ta}/(\text{Ta} + \text{Nb})$ | 0.09 | 0.08 | 0.00 | 0.03 | 0.09 | 0.00 | 0.05 | 0.04 |

b.d.l.—below detection limit.

#### 4.3.2. Columbite-Group Minerals

Columbite-group minerals in both varieties of high-F, high- $\text{P}_2\text{O}_5$  Li-mica granites occur mostly as euhedral to subhedral grains. Some grains display irregular or patched zoning (Figure 4). No systematic core-rim compositional evolution was observed. The columbite-group minerals are represented predominantly by columbite-(Fe) with a  $\text{Mn}/(\text{Mn} + \text{Fe})$  ratio varying from 0.07 to 0.15 and with relatively low  $\text{Ta}/(\text{Ta} + \text{Nb})$  values (0.06–0.41) (Table 3).

**Table 3.** Representative microprobe analyses of columbite-group minerals (wt %).

| Sample                  | 971-6 | 971-11 | 971-14 | 1543-44 | 1543-45 | 1543-47 | 1543-48 |
|-------------------------|-------|--------|--------|---------|---------|---------|---------|
| $\text{WO}_3$           | 2.24  | 2.17   | 1.60   | 4.52    | 2.10    | 3.88    | 5.41    |
| $\text{Ta}_2\text{O}_5$ | 28.36 | 25.92  | 32.70  | 33.68   | 20.16   | 24.20   | 19.31   |
| $\text{Nb}_2\text{O}_5$ | 47.79 | 45.73  | 43.41  | 40.66   | 52.96   | 47.10   | 49.45   |
| $\text{TiO}_2$          | 2.22  | 4.57   | 2.26   | 2.26    | 4.31    | 4.93    | 4.84    |
| $\text{SiO}_2$          | 0.00  | 0.02   | 0.00   | 0.02    | 0.05    | 0.04    | 0.03    |
| $\text{ZrO}_2$          | 0.07  | 0.38   | 0.15   | 0.29    | 0.64    | 0.23    | 0.20    |
| $\text{SnO}_2$          | 0.28  | 1.29   | 0.50   | 1.15    | 0.99    | 1.66    | 1.39    |
| $\text{Al}_2\text{O}_3$ | 0.01  | 0.03   | 0.02   | 0.00    | 0.00    | 0.00    | 0.03    |
| $\text{Y}_2\text{O}_3$  | 0.10  | 0.19   | 0.17   | 0.12    | 0.07    | 0.05    | 0.11    |
| $\text{Sc}_2\text{O}_3$ | 0.19  | 0.29   | 0.39   | 0.02    | 0.15    | 0.08    | 0.07    |
| $\text{Fe}_2\text{O}_3$ | 0.29  | 1.29   | 0.98   | 0.49    | 1.18    | 0.42    | 0.83    |
| $\text{FeO}$            | 16.57 | 16.12  | 15.07  | 15.62   | 15.42   | 15.78   | 16.17   |
| $\text{MnO}$            | 1.40  | 1.56   | 2.02   | 1.80    | 1.93    | 1.61    | 1.66    |
| $\text{CaO}$            | 0.01  | 0.01   | 0.00   | 0.00    | 0.00    | 0.10    | 0.00    |
| Total                   | 99.53 | 99.57  | 99.27  | 100.63  | 99.96   | 100.08  | 99.50   |
| O = 6, apfu             |       |        |        |         |         |         |         |
| $\text{W}^{6+}$         | 0.04  | 0.04   | 0.03   | 0.08    | 0.03    | 0.06    | 0.09    |
| $\text{Ta}^{5+}$        | 0.49  | 0.44   | 0.58   | 0.60    | 0.33    | 0.41    | 0.32    |
| $\text{Nb}^{5+}$        | 1.37  | 1.30   | 1.27   | 1.20    | 1.45    | 1.32    | 1.37    |
| $\text{Ti}^{4+}$        | 0.11  | 0.22   | 0.11   | 0.11    | 0.20    | 0.23    | 0.22    |
| $\text{Si}^{4+}$        | 0.00  | 0.00   | 0.00   | 0.00    | 0.00    | 0.00    | 0.00    |
| $\text{Zr}^{4+}$        | 0.00  | 0.01   | 0.01   | 0.01    | 0.02    | 0.01    | 0.01    |
| $\text{Sn}^{4+}$        | 0.01  | 0.03   | 0.01   | 0.03    | 0.02    | 0.04    | 0.03    |
| $\text{Al}^{3+}$        | 0.00  | 0.00   | 0.00   | 0.00    | 0.00    | 0.00    | 0.00    |
| $\text{Y}^{3+}$         | 0.00  | 0.01   | 0.01   | 0.00    | 0.00    | 0.00    | 0.00    |
| $\text{Sc}^{3+}$        | 0.01  | 0.02   | 0.02   | 0.00    | 0.01    | 0.00    | 0.00    |
| $\text{Fe}^{3+}$        | 0.01  | 0.06   | 0.05   | 0.02    | 0.05    | 0.02    | 0.04    |
| $\text{Fe}^{2+}$        | 0.88  | 0.79   | 0.82   | 0.85    | 0.78    | 0.82    | 0.83    |
| $\text{Mn}^{2+}$        | 0.08  | 0.08   | 0.11   | 0.10    | 0.10    | 0.08    | 0.09    |
| $\text{Ca}^{2+}$        | 0.00  | 0.00   | 0.00   | 0.00    | 0.00    | 0.01    | 0.00    |

|              |      |      |      |      |      |      |      |
|--------------|------|------|------|------|------|------|------|
| Total        | 3.00 | 3.00 | 3.00 | 3.00 | 3.00 | 3.00 | 3.00 |
| Mn/(Mn + Fe) | 0.08 | 0.10 | 0.12 | 0.11 | 0.11 | 0.09 | 0.09 |
| Ta/(Ta + Nb) | 0.26 | 0.25 | 0.31 | 0.33 | 0.19 | 0.24 | 0.19 |

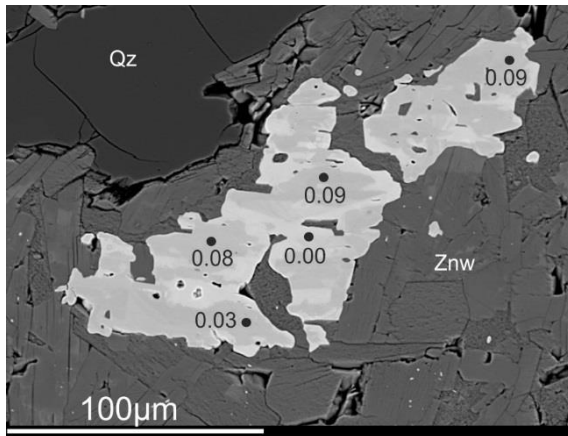


**Figure 3.** BSE image of zoned Nb-Ta-rich rutile showing variation in  $\text{Ta}/(\text{Ta} + \text{Nb})$  ratio. Qz—quartz, Znw—Li-mica.

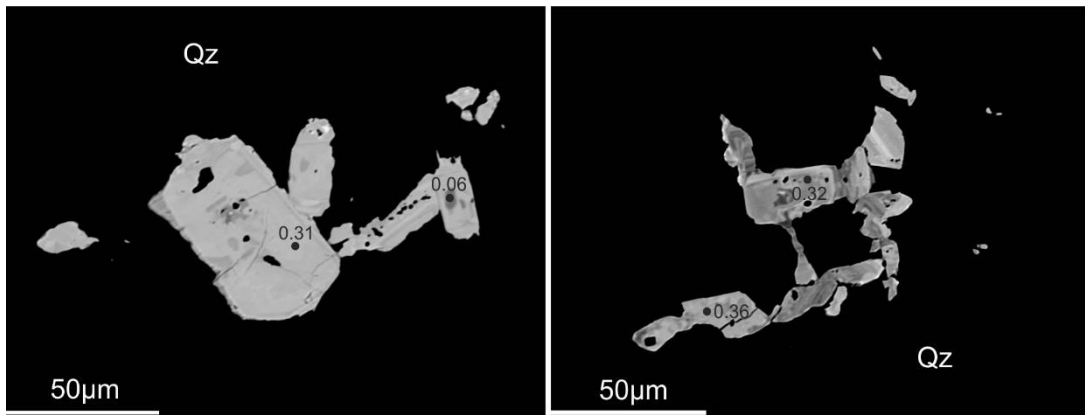


**Figure 4.** BSE images of zoned columbite-(Fe) showing variation in  $\text{Ta}/(\text{Ta} + \text{Nb})$  ratio. Qz—quartz.

#### 4.3.3. Ixiolite

In this paper the term ixiolite is used to describe minerals of columbite-like chemical composition and W content greater than 0.10 apfu. However, structural data confirming the identity of this mineral are not available. The W-bearing ixiolite was observed as needle-like subhedral crystals occurring in fine-grained aplitic granite from the intrusive breccias (Figure 5). The ixiolite is Fe-rich with relatively low  $\text{Mn}/(\text{Mn} + \text{Fe})$  and  $\text{Ta}/(\text{Ta} + \text{Nb})$  values (0.10–0.15 and 0.06–0.20 respectively. Owing to the high W content (19.8–34.9 wt %  $\text{WO}_3$ , 0.11–0.20 apfu), the sum of Nb + Ta in the ixiolite does not exceed 0.43 apfu. The Ti content is 1.7–5.7 wt %  $\text{TiO}_2$  and Sn content is relatively low (0.3–4.1 wt %  $\text{SnO}_2$ ) (Table 4).

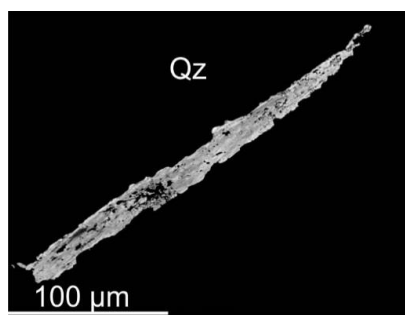


**Figure 5.** BSE image of W-bearing ixiolite. Qz-quartz.

**Table 4.** Representative microprobe analyses of ixiolite (wt %).

| Sample                         | 1705-16 | 1705-19 | 1705-20 | 1705-28 | 1706-54 |
|--------------------------------|---------|---------|---------|---------|---------|
| WO <sub>3</sub>                | 34.89   | 29.20   | 32.06   | 23.76   | 19.81   |
| Ta <sub>2</sub> O <sub>5</sub> | 3.44    | 3.79    | 4.86    | 4.72    | 14.28   |
| Nb <sub>2</sub> O <sub>5</sub> | 31.24   | 37.70   | 31.31   | 42.13   | 34.37   |
| TiO <sub>2</sub>               | 1.69    | 2.03    | 1.72    | 2.35    | 5.68    |
| SiO <sub>2</sub>               | 0.16    | 0.24    | 0.18    | 0.11    | 0.02    |
| ZrO <sub>2</sub>               | 0.59    | 0.64    | 0.56    | 0.64    | 0.84    |
| SnO <sub>2</sub>               | 0.33    | 0.33    | 0.35    | 0.32    | 4.13    |
| UO <sub>2</sub>                | 0.05    | 0.05    | b.d.l.  | 0.07    | b.d.l.  |
| Al <sub>2</sub> O <sub>3</sub> | 0.32    | 0.47    | 0.25    | 0.13    | 0.01    |
| Y <sub>2</sub> O <sub>3</sub>  | b.d.l.  | b.d.l.  | b.d.l.  | b.d.l.  | 0.01    |
| Sc <sub>2</sub> O <sub>3</sub> | 0.09    | 0.10    | 0.08    | 0.10    | 0.31    |
| Bi <sub>2</sub> O <sub>3</sub> | 0.33    | 0.49    | 0.28    | 0.32    | 0.06    |
| Fe <sub>2</sub> O <sub>3</sub> | 3.26    | 3.07    | 3.24    | 2.51    | 0.97    |
| FeO                            | 15.28   | 15.36   | 15.35   | 15.69   | 16.40   |
| MnO                            | 2.88    | 2.91    | 2.99    | 3.09    | 1.84    |
| MgO                            | 0.04    | 0.07    | 0.02    | 0.04    | b.d.l.  |
| CaO                            | 0.18    | 0.21    | 0.08    | 0.06    | b.d.l.  |
| Total                          | 94.77   | 96.66   | 93.33   | 96.04   | 98.73   |
| O = 2, apfu                    |         |         |         |         |         |
| W <sup>6+</sup>                | 0.20    | 0.16    | 0.19    | 0.13    | 0.11    |
| Ta <sup>5+</sup>               | 0.02    | 0.02    | 0.03    | 0.03    | 0.08    |
| Nb <sup>5+</sup>               | 0.32    | 0.37    | 0.32    | 0.41    | 0.33    |
| Ti <sup>4+</sup>               | 0.03    | 0.03    | 0.03    | 0.04    | 0.09    |
| Si <sup>4+</sup>               | 0.00    | 0.01    | 0.00    | 0.00    | 0.00    |
| Zr <sup>4+</sup>               | 0.01    | 0.01    | 0.01    | 0.01    | 0.01    |
| U <sup>4+</sup>                | 0.00    | 0.00    | 0.00    | 0.00    | 0.00    |
| Al <sup>3+</sup>               | 0.01    | 0.01    | 0.01    | 0.00    | 0.00    |
| Y <sup>3+</sup>                | 0.00    | 0.00    | 0.00    | 0.00    | 0.00    |
| Sc <sup>3+</sup>               | 0.00    | 0.00    | 0.00    | 0.00    | 0.01    |
| Bi <sup>3+</sup>               | 0.00    | 0.00    | 0.00    | 0.00    | 0.00    |
| Fe <sup>3+</sup>               | 0.07    | 0.06    | 0.07    | 0.05    | 0.02    |
| Fe <sup>2+</sup>               | 0.34    | 0.33    | 0.35    | 0.32    | 0.31    |
| Mn <sup>2+</sup>               | 0.06    | 0.05    | 0.06    | 0.06    | 0.03    |
| Mg <sup>2+</sup>               | 0.00    | 0.00    | 0.00    | 0.00    | 0.00    |
| Ca <sup>2+</sup>               | 0.00    | 0.01    | 0.00    | 0.00    | 0.00    |
| Total                          |         |         |         |         |         |
| Mn/(Mn + Fe)                   | 0.14    | 0.14    | 0.14    | 0.15    | 0.10    |
| Ta/(Ta + Nb)                   | 0.06    | 0.06    | 0.09    | 0.06    | 0.20    |

b.d.l.—below detection limit.

## 5. Discussion

Columbite group minerals together with Nb-Ta-rich rutile are important accessory minerals in highly fractionated granitic rocks. The presence of Nb and Ta in rutile is commonly interpreted to indicate a solid solution between TiO<sub>2</sub> and (Fe, Mn)(Nb, Ta)<sub>2</sub>O<sub>6</sub> [24]. The solubility of rutile in magmas varies significantly with the nature of the melt. However, its solubility in peraluminous granites is very low [25,26]. Enrichment of Ta and consequently, low whole-rock Nb/Ta values were found in highly peraluminous granites from the Beauvoir stock in France [27,28], Yichun complex in China

[29] and Limu complex in China [30]. According Ballouard et al. [31] the ratio  $\text{Nb}/\text{Ta} = 5$  appears to be a good marker to discriminate mineralized from barren peraluminous granites (Figure 6).

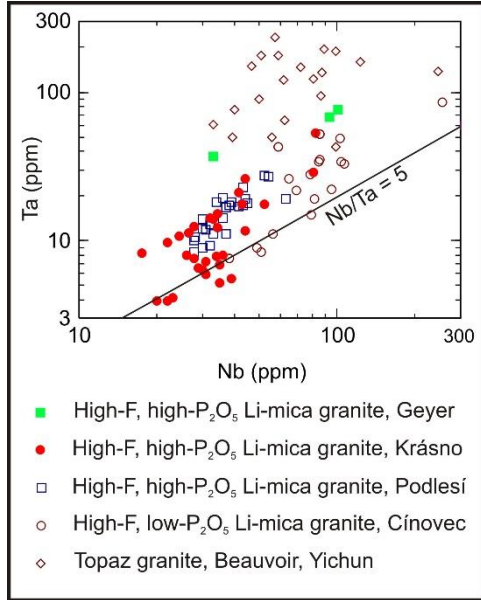


**Figure 6. Ta vs. Nb concentrations in high-F, high-P<sub>2</sub>O<sub>5</sub> Li-mica granites and related rocks.**

In comparison with the above mentioned localities, the high-F, high-P<sub>2</sub>O<sub>5</sub> Li-mica granites from the Geyersberg, Krásno-Horní Slavkov ore district [5] (René and Škoda 2011), Podlesí [32] and the high-F, low P<sub>2</sub>O<sub>5</sub> Li-mica granites from the Cínovec granite cupola [2,33] show a lower degree of granite fractionation and consequently, higher Nb/Ta ratio. The Nb enrichment of these granites very probably reflects a partly different nature of the protolith [34].

In all of these highly fractionated granites, Nb and Ta are predominantly hosted in Nb-Ta-rich rutile and to a lesser extent in columbite-group minerals [1–4,35]. The columbite-group minerals from the Geyersberg and Podlesí [4] granite stocks display relative low Mn/(Mn + Fe) ratio, ranging from 0.07 to 0.2. The columbite-group minerals from the Krásno-Horní Slavkov district [1] (René and Škoda 2011) and the Cínovec granite cupola [1–3] have a highly variable Mn/(Mn + Fe) ratio, ranging from 0.15 to 0.9. A similarly wide variation has been observed in highly fractionated granites from the Cornwall and Beauvoir [35,36]. The highest Mn/(Mn + Fe) ratio was found in columbite-group minerals from the Yichun granite stock [35] (Figure 7). The increase of Mn/(Mn + Fe) ratio in columbite-group minerals is attributed to fractional crystallisation in mineralised granites [35,37]. Experiments show that the solubility of columbite-(Mn) is significantly controlled by the aluminium saturation index (AS), Li and P concentrations [38,39].

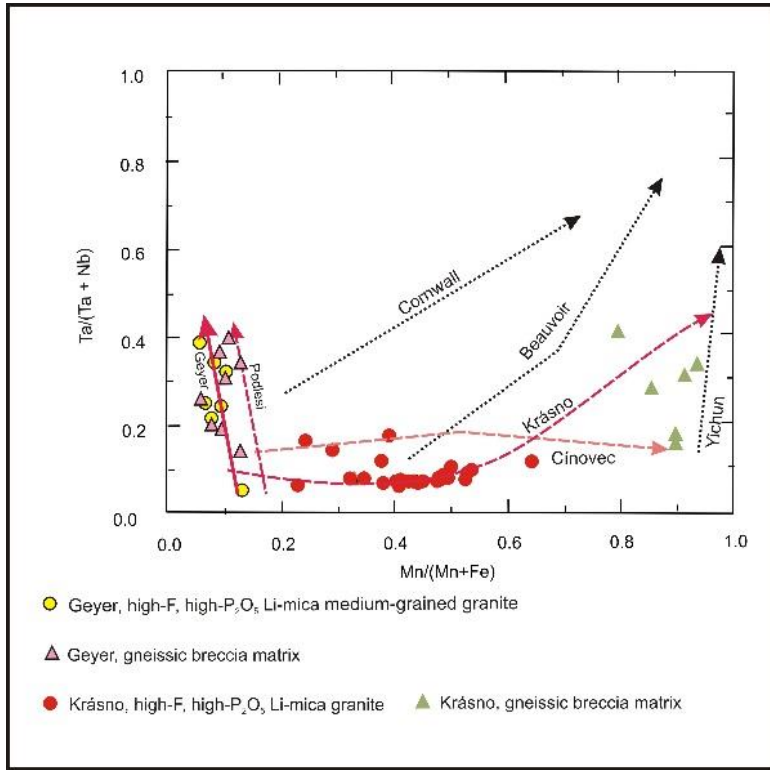


**Figure 7.** Schematic Ta/(Ta + Nb) vs. Mn/(Mn + Fe) composition plot for columbite-group minerals from high-F, high-P<sub>2</sub>O<sub>5</sub> Li mica granites and related rocks.

The W-bearing ixiolite, which was found as a scarce mineral phase in fine-grained aplitic granites occurring as a matrix of intrusive breccias display low Mn/(Mn + Fe) ratio (0.10–0.15). Similar ixiolite was also found as relative scarce mineral phase in high-F granites from the Hub stock in the Krásno-Horní Slavkov ore district [5], Podlesí granite stock [4] and Cínovec granite cupola [1,3]. Ixiolite from the Hub and Podlesí granite stock and from the Cínovec granite cupola displays higher Mn/(Mn + Fe) ratio (0.14–0.37). The Ta/(Nb + Ta) ratio in ixiolite from the Geyersberg is relatively low (0.06–0.20), whereas the Ta/(Nb + Ta) ratio in ixiolite from the Podlesí granite stock and the Cínovec cupola is higher (0.14–0.50).

## 6. Conclusions

The Nb-Ta-rich rutile and columbite-group minerals and W-bearing ixiolite represent significant accessory minerals in granitic rocks of the Geyersberg granite stock. The high-F, high-P<sub>2</sub>O<sub>5</sub> Li-mica Geyersberg granites are highly fractionated S-type granites (ASI = 1.2–1.5) with low Nb/Ta ratio (0.9–1.4). Columbite-group minerals are represented by columbite-(Fe) with Mn/(Mn + Fe) ratio ranging from 0.07 to 0.15. The rare Fe-rich W-bearing ixiolite occurs as small needle-like crystals. The ixiolite is Fe-rich with relatively low Mn/(Mn + Fe) and Ta/(Ta + Nb) values (0.10–0.15 and 0.06–0.20 respectively).

**Acknowledgments:** The research for this paper was carried out thanks to the support of the long-term conceptual development research organisation RVO 67985891. P. Gadas and R. Škoda from the Masaryk University, Brno are thanked for their assistance during the microprobe work. I am also grateful to P. Voudouris for numerous helpful comments and recommendations which helped to improve this paper.

**Conflict of Interest:** The author declares no conflict of interest.

## References

1. Johan, Z.; Johan, V. Accessory minerals of the Cínovec (Zinnwald) granite cupola, Czech Republic. Part 1: Nb-, Ta- and Ti-bearing oxides. *Mineral. Petrol.* **1994**, *83*, 113–150, doi:10.1007/s00710-004-0058-0
2. Rub, A.K.; Štemprok, M.; Rub, M.G. Tantalum mineralisation in the apical part of the Cínovec (Zinnwald) granite stock. *Mineral. Petrol.* **1998**, *63*, 199–222, doi:10.1007/BF01164151
3. Breiter, K.; Korbelová, Z.; Chládek, Š.; Uher, P.; Kněsl, I.; Rambousek, P.; Honig, S.; Šešulka, V. Diversity of Ti-Sn-Nb-Ta oxide minerals in the classic granite related magmatic-hydrothermal Cínovec/Zinnwald Sn-W-Li deposit (Czech Republic). *Eur. J. Mineral.* **2017**, *29*, 727–738, doi:10.1127/ejm/2017/0029-2650
4. Breiter, K.; Škoda, R.; Uher, P. Nb-Ta-Ti-W-Sn-oxide minerals as indicators of a peraluminous P- and F-rich granitic system evolution: Podlesí, Czech Republic. *Mineral. Petrol.* **2007**, *91*, 225–248, doi:10.1007/s0710-007-0197-1
5. René, M.; Škoda, R. Nb-Ta-Ti oxides fractionation in rare-metal granites: Krásno-Horní Slavkov ore district, Czech Republic. *Mineral. Petrol.* **2011**, *103*, 37–48, doi:10.1007/s00710-011-0152-z
6. Förster, H.J.; Tischendorf, G.; Trumbull, R.B.; Gottesmann, B. Late-collisional granites in the Variscan Erzgebirge (Germany). *J. Petrol.* **1999**, *40*, 1613–1645, doi:10.1093/petroj/40.11.1613
7. Romer, R.L.; Thomas, R.; Stein, H.J.; Rhede, D. Dating multiply overprinted Sn-mineralized granites—Examples from the Erzgebirge, Germany. *Mineral. Deposita* **2007**, *42*, 337–359, doi:10.1007/s00126-006-0114-2
8. Tichomirova, M.; Leonhardt, D. New age determinations (Pb-Pb zircon evaporation, Rb/Sr) on the granites from Aue-Scharzenberg and Eibenstock, Western Erzgebirge, Germany. *Z. Geol. Wiss.* **2010**, *38*, 99–123.
9. Hofmann, Y.; Jahr, T.; Jentzsch, G. Three-dimensional gravimetric modelling to detect deep structure of the region Vogtland/NW Bohemia. *J. Geodyn.* **2003**, *35*, 209–220, doi:10.1016/s0264-3707(02)00063-7
10. Blecha, V.; Štemprok, M. Petrochemical and geochemical characteristics of late Variscan granites in the Karlovy Vary Massif (Czech Republic)—Implications for gravity and magnetic interpretation at shallow depths. *J. Geosci.* **2012**, *57*, 65–85.
11. Fiala, F. Granitoids of the Slavkovský (Císařský) les Mountains. *Sbor. Geol. Věd. G* **1968**, *14*, 93–160.
12. Tischendorf, G. Zur geochemischen Spezialisierung der Granite des westerzgebirgischen Teilplutons. *Geologie* **1970**, *19*, 25–40.
13. Lange, H.; Tischendorf, G.; Pälchen, W.; Klemm, I.; Ossenkopf, W. Zur Petrographie und Geochemie der Granite des Erzgebirges. *Geologie* **1972**, *21*, 457–492.
14. Kaemmel, T.; Just, G. Geochemical differentiation of granitoids in the G.D.R. using normalized trace element differences. *Gerlands Beitr. Geophysik* **1985**, *94*, 351–369.
15. Štemprok, M. Petrology and geochemistry of the Czechoslovak part of the Krušné hory Mts. *Sbor. Geol. Věd. LG* **1986**, *27*, 111–156.
16. Tischendorf, G.; Geisler, M.; Gerstenberger, H.; Budzinski, H.; Vogler, P. Geochemistry of Variscan granites of the Westerzgebirge Vogtland region—An example of tin deposit-generating granites. *Chem. Erde* **1987**, *46*, 213–235.
17. Förster, H.J.; Römer, R.L. Carboniferous magmatism. In *Pre-Mesozoic Geology of Saxo-Thuringia—From the Cadomian Active Margin to the Varisan Orogen*; Linnemann, U., Romer, R.L., Eds.; Schweizerbart Verlag: Stuttgart, Germany, 2010; pp. 287–308.
18. Höth, K.; Ossenkopf, W.; Hösel, G.; Zernke, B.; Eisenschmidt, K.; Kühne, R. Die Granite im Westteil des Mittelerzgebirgischen Teilplutons und ihr Rahmen. *Geoprofil* **1991**, *3*, 3–13.
19. Hösel, G.; Höth, K.; Jung, D.; Leonhardt, D.; Mann, M.; Meyer, H.; Tägl, U. Das Zinnerz-Lagerstättengebiet Ehrenfriedersdorf/Erzgebirge. *Bergbau Sachsen* **1994**, *1*, 1–196.
20. Hösel, G.; Fritsch, E.; Josiger, U.; Wolf, P. Das Lagerstättengebiet Geyer. *Bergbau Sachsen* **1996**, *4*, 1–112.
21. Tischendorf, G.; Wasternack, J.; Bolduan, H.; Bein, E. Zur Lage der Granitoberfläche im Erzgebirge und Vogtland mit Bemerkungen über ihre Bedeutung für die Verteilung endogener Lagerstätten. *Z. Angew. Geol.* **1965**, *11*, 410–423.
22. Pouchou, J.L.; Pichoir, F. “PAP” ( $\phi$ - $q$ -Z) procedure for improved quantitative microanalysis. In *Microbeam Analysis*; Armstrong, J.T., Ed.; San Francisco Press: San Francisco, CA, USA, 1985; pp. 104–106.
23. Chappell, B.W.; Hine, R. The Cornubian batholith: An example of magmatic fractionation on a crustal scale. *Res. Geol.* **2006**, *56*, 203–244, doi:10.1111/j.1751-3928.2006.tb00281.x
24. Černý, P.; Ercit, T.S. Some recent advances in the mineralogy and geochemistry of Nb and Ta in rare-element granitic pegmatites. *Bull. Minéral.* **1985**, *108*, 499–532.

25. Ryerson, F.J.; Watson, E.B. Rutile saturation in magmas: Implications for Ti-Nb-Ta depletion in island-arc basalts. *Earth Planet Sci. Lett.* **1987**, *86*, 225–239, doi:10.1016/0012-821x(87)90223-8
26. Keppler, H. Influence of fluorine on the enrichment of high-field-strength trace elements in granitic rocks. *Contrib. Miner. Petrol.* **1993**, *114*, 479–488, doi:10.1007/BF00321752
27. Raimbault, L.; Cuney, M.; Azencott, C.; Duthou, J.L.; Joron, J.L. Geochemical evidence for a multistage genesis of Ta-Sn-Li mineralization in the granite at Beauvoir, French Massif Central. *Econ. Geol.* **1995**, *90*, 548–576, doi:10.2113/gsecongeo.90.3.548
28. Breiter, K.; Škoda, R. Vertical zonality of fractionated granite plutons reflected in zircon chemistry: The Cínovec A-type versus the Beauvoir S-type suite. *Geol. Carpath.* **2012**, *63*, 383–398, doi:10.2478/v10096-012-0030-6
29. Huang, X.L.; Wang, R.C.; Chen, X.M.; Hu, H.; Liu, C.S. Vertical variations in the mineralogy of the Yichun topaz-lepidolite granite, Jiangxi province, South Chiuna. *Can. Miner.* **2002**, *40*, 1047–1068, doi:10.2113/gscanmin.40.4.1047
30. Zhu, J.C.; Li, R.K.; Li, F.C.; Xiong, X.L.; Zhou, F.Y.; Huang, X.L. Topaz-albite granites and rare-metal mineralization in the Limu district, Guangxi province, southeast China. *Mineral. Deposita* **2001**, *36*, 393–405, doi:10.1007/s001260100160
31. Ballouard, C.; Poujol, M.; Boulvais, P.; Branquet, Y.; Tartèse, R.; Vigneresse, J.L. Nb-Ta fractionation in peraluminous granites: A marker of the magmatic-hydrothermal transition. *Geology* **2016**, *44*, 231–234, doi:10.1130/G37475.1
32. Breiter, K. From explosive breccia to inidirectional solidification textures: Magmatic evolution of a phosphorus- and fluorine-rich granite system (Podlesí, Krušné hory Mts., Czech Republic). *Bull. Czech Geol. Surv.* **2002**, *77*, 67–72.
33. Breiter, K.; Ďurišová, J.; Hrstka, T.; Korbelová, Z.; Hložková Vaňková, M.; Vašinová Galiová, M.; Rambousek, P.; Kněsl, I.; Dobeš, P.; Dosbaba, M. Assessment of magmatic vs. metasomatic processes in rare-metal granites: A case study of the Cínovec/Zinnwald Sn-W-Li deposit, Central Europe. *Lithos* **2017**, 292–293, 198–217, doi:10.1016/j.lithos.2017.08.015
34. Breiter, K. Nearly contemporaneous evolution of the A- and S-type fractionated granites in the Krušné hory/Erzgebirge Mts., Central Europe. *Lithos* **2012**, *151*, 105–121, doi:10.1016/j.lithos.2011.09.022
35. Belkasmi, M.; Cuney, M.; Polard, P.J.; Bastoul, A. Chemistry of the Ta-Nb-Sn-W oxide minerals from the Yichun rare metal granite (SE China): Genetic implications and comparison with Moroccan and French Hercynian examples. *Miner. Mag.* **2000**, *64*, 507–533, doi:10.1180/002646100549391
36. Scott, P.W.; Pascoe, R.D.; Hart, F.W. Columbite-tantalite, rutile and other accessory minerals from the St. Austell topaz granite, Cornwall. *Geosci. South-West Engl.* **1998**, *9*, 165–170.
37. Linnen, R.L.; Cuney, M. Granite-related rare-element deposits and experimental constraints on Ta-Nb-W-Sn-Zr-Hf mineralization. In *Rare-Element Geochemistry and Mineral Deposits*; Linnen, R.L., Samson, I.M., Eds.; *Can. Short Courses Notes* **2005**, *17*, 45–67.
38. Linnen, R.L. The solubility of Nb-Ta-Zr-Hf-W in granitic melts with Li and Li+F: Constraints for mineralization in rare-metal granites and pegmatites. *Econ. Geol.* **1998**, *93*, 1013–1025, doi:10.2113/gsecongeo.93.7.1013
39. Fiege, A.; Kirchner, C.; Barthels, A.; Holtz, F.; Linnen, R.L. Influence of fluorine on the solubility of manganotantalite ( $MnTa_2O_6$ ) and manganocolumbite ( $MnNb_2O_6$ ) in natural rhyolitic, synthetic haplogranitic and pegmatitic melts. *Hall. Jahrb. Geowiss.* **2009**, *31*, 60.



© 2018 by the authors. Licensee MDPI, Basel, Switzerland. This article is an open access article distributed under the terms and conditions of the Creative Commons by Attribution (CC-BY) license (<http://creativecommons.org/licenses/by/4.0/>).